JOURNAL OF SOLID STATE CHEMISTRY 63, 70–75 (1986)

Crystal Structure of $Bi_2Mo_2O_9$: A Selective Oxidation Catalyst

HORNG-YIH CHEN AND ARTHUR W. SLEIGHT[1]

Central Research and Development Department,[2] E. I. duPont de Nemours and Company, Experimental Station, Wilmington, Delaware 19898

Received August 2, 1985; in revised form October 16, 1985

$Bi_2Mo_2O_9$ is monoclinic; space group $P2_1/n$ with $a = 11.972(3)$ Å, $b = 10.813(4)$ Å, $c = 11.899(2)$, $\beta = 90.13(2)$, and $Z = 8$. The structure was solved by Patterson and Fourier techniques. The final agreement factors of the refinement based on 2711 independent reflections were $R = 0.051$ and $R_w = 0.057$. Based on the structure, the formula may be represented as $Bi(Bi_3O_2)(MoO_4)_4$. There are Bi_3O_2 chains parallel to the b-axis. There are also Bi atoms bound only to MoO_4 tetrahedra. Contrary to earlier reports, the isolated MoO_4 tetrahedra are very regular.

Introduction

Molybdates are unsurpassed as selective oxidation catalysts for reactions such as methanol oxidation to formaldehyde and propylene ammoxidation to acrylonitrile (*1*). We have recently shown that ferric molybdate, a frequent component of such catalysts, contains highly regular MoO_4 tetrahedra (*2*). Now we find the same feature in $Bi_2Mo_2O_9$.

Of the bismuth molybdates, the three phases showing simultaneously high activity and selectivity for the partial oxidation of hydrocarbons are Bi_2MoO_6, $Bi_2Mo_2O_9$, and $Bi_2Mo_3O_{12}$. The structures of Bi_2MoO_6 and $Bi_2Mo_3O_{12}$ are known (*3, 4*). However, current evidence is that the best catalyst among these bismuth molybdates is $Bi_2Mo_2O_9$ (*5*), and this structure has been controversial. Good single crystals have not been available, and a totally reliable structure has not been reported.

van der Elzen and Rieck (*6*) published a structure for $Bi_2Mo_2O_9$ based on X-ray powder data. They approximated the monoclinic $P2_1/n$ cell as an orthorhombic *Pmnb* cell and reported only metal positions. Although unable to locate the oxygen atoms, they suggested positions assuming distorted MoO_4 tetrahedral coordination. Based on spectroscopic evidence, Haber and co-workers (*7*) concluded that the molybdenum coordination in $Bi_2Mo_2O_9$ is mixed octahedral and tetrahedral. We have now obtained a suitable crystal of $Bi_2Mo_2O_9$, and an accurate structure is reported for the first time.

Sample Preparation

The $Bi_2Mo_2O_9$ sample was prepared from a mixture of Bi_2O_3 (Baker, Reagent Grade) and MoO_3 (Matheson, Coleman and Bell) of mole ratio 27.5/72.5. The mixture was

[1] To whom correspondence should be addressed.

[2] Contribution No. 3017.

0022-4596/86 $3.00

melted at 700°C in a Pt–Rh crucible. A crystal pulled by the Czochralski method at 670°C using a Pt/20%-Rh wire rotating at 60 rmp was severely twinned. However, clear yellow fragments were isolated that showed diffraction patterns of a pseudoorthorhombic phase with $a = 11.949$ Å, $b = 10.795$ Å, and $c = 11.877$ Å. Several crystal fragments were examined by X-ray methods before a single crystal suitable for structure work was obtained.

X-Ray Data Collection

A clear crystal, approximately $0.1 \times 0.033 \times 0.033$ mm, was mounted with the needle axis making roughly a 45° angle with the spindle axis. Preliminary examination by the precession technique indicated the crystal was single and probably has orthorhombic symmetry as reported by Erman *et al.* (*8*). When examinations were carried out with a Syntex P3 diffractometer, the axial photographs with extended exposure time showed violations of mirror symmetry for two of the three orthorhombic axes. Thus, it was concluded that the structure belonged to a monoclininc rather than an orthorhombic system. With 25 reflections and their Friedel pairs, the lattice parameters at 25°C were refined to $a = 11.972(3)$ Å, $b = 10.813(4)$ Å, $c = 11.899(2)$ Å, and $\beta = 90.13°(2)$. From fast-scan data, the nonextinction conditions were found to be ($h0l$): $h + l = 2n$, and ($0k0$): $k = 2n$. This indicated space group $P2_1/n$, in agreement with van der Elzen and Rieck (*5*).

Intensity data were collected at room temperature using the Syntex diffractometer (graphite monochromator, Mo$K\alpha$ radiation, $\lambda = 0.7107$ Å) and the ω-scan method. Because of the small crystal size, data were collected at relatively slow scan rates, 1.5 to 3°/min with the X-ray tube operated at the maximum output of 2400 W. The scan range was 1° with the background time equal to scan time. From ψ-scan data of four reflections with 2θ ranging from 8.51 to 44.63°, the normalized transmission coefficients varied from 52 to 100%. Accordingly, an empirical absorption correction was carried out for the intensities using the ψ-scan data. Totally, 5708 reflections were measured in the range of $0° < 2\theta < 50°$ (for the hemisphere $\pm h$, k, $\pm l$); after averaging, 2711 independent reflections were obtained. The output from the averaging program showed that the equivalent reflections indeed had the same intensities within the experimental error. The data were not complicated by twinning.

Structure Determination and Refinements

Solution and refinements of the structure were accomplished on a PDP-11 computer, using local modifications of the structure determination package supplied by the Enraf-Nonius Corporation (*9*). The atomic scattering factors were taken from the tabulations of Cromer and Waber (*10*). Anomalous dispersion corrections were Cromer (*10*). In the full-matrix least-squares refinement, the function minimized was $\Sigma w(|F_o| - |F_c|)^2$, where the weight, w, was the reciprocal of the value of $\sigma(F^2) + 0.02\,F^2$.

From the E statistics of the data, the $\langle E \rangle$ values are all very small for $k = 2n + 1$, indicating a very strong subcell character in the b-direction. Furthermore, the entire data depicted roughly a body-centered tetragonal cell with $a° = a/3$, $b° = c/3$, and $c° = b/2$. With the strong subcell nature, the direct method could not yield a satisfactory solution for positioning the heavy metal atoms. The Patterson map of the entire cell produced 36 distinct peaks, only 32 of which should represent the metal atoms in the actual structure. In order to locate the origin and, at the same time, exclude the four unoccupied sites, the 36 Patterson peaks were compared with the 32 atom positions proposed by van der Elzen *et al.* (*6*). It was found that if their 32 positions were to be consistent with the space group $P2_1/n$, the origin should be located at ($\frac{3}{4}$, $\frac{1}{8}$, $\frac{1}{4}$) and

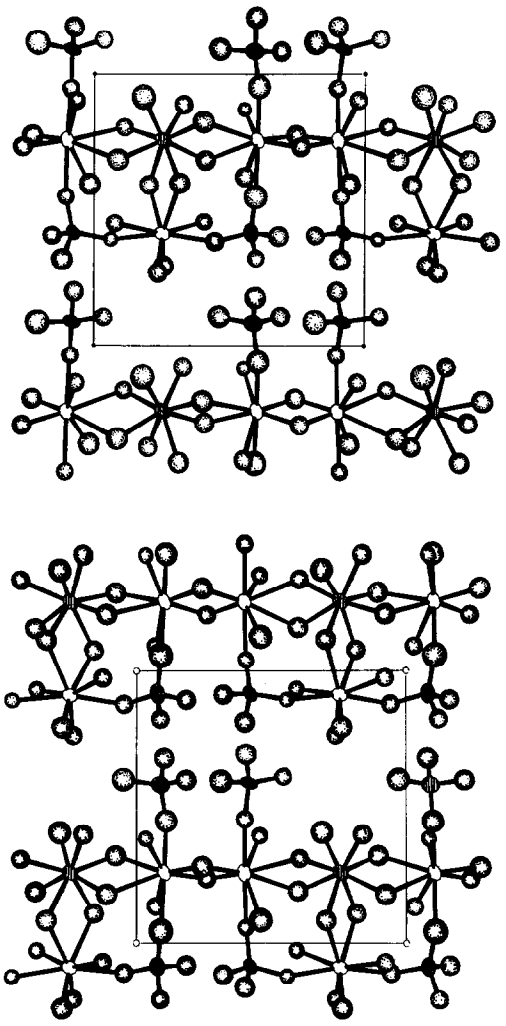

FIG. 1. Structure of $Bi_2Mo_2O_9$ projected in the a–c plane. The unit cell is outlined with a as the horizontal axis. Oxygen atoms are shaded. Molybdenum is tetrahedrally coordinated, and bismuth is eight-coordinated. The upper and lower sections are at about $z = \frac{1}{8}$ and $\frac{3}{8}$, respectively.

the 2_1 screw axis at $(0, y, \frac{1}{2})$. With this assignment of the origin, the 32 positions could be represented by the following eight independent atoms

Bi(1) at $(-\frac{1}{12}, \frac{1}{8}, \frac{3}{4})$
Bi(2) at $(\frac{7}{12}, \frac{1}{8}, \frac{3}{4})$
Bi(3) at $(\frac{1}{4}, \frac{1}{8}, \frac{3}{4})$
Bi(4) at $(\frac{1}{4}, \frac{1}{8}, \frac{5}{12})$
Mo(1) at $(-\frac{1}{12}, \frac{1}{8}, \frac{1}{12})$
Mo(2) at $(-\frac{1}{12}, \frac{1}{8}, \frac{5}{12})$
Mo(3) at $(\frac{7}{12}, \frac{1}{8}, \frac{1}{12})$
Mo(4) at $(\frac{7}{8}, \frac{1}{8}, \frac{5}{12})$

Refinements with the 8 metal atoms led to an R of 0.18. Subsequently, 13 O atoms were positioned from the difference Fourier map and refined convergently. Peaks for the remaining 5 oxygens were not found. At this stage, it was assumed that all the Mo atoms had an ideal MoO_4 tetrahedral coordination and the positions of missing O atoms were calculated. Subsequent refinements quickly converged to an R of 0.062. Finally, the thermal parameters of the metal atoms were refined anisotropically, and $R = 0.051$ and $R_w = 0.057$ were obtained. The maximum residual electron density in the difference Fourier map was about 1.0 $e^-/Å^3$. Conversion from iso- to anisotropic thermal parameters for O atoms did not improve the refinement, and the refinements involving the multiplicity for the metal atoms failed to show any degree of partial occupancy. It was, therefore, concluded that the correct formula was indeed $Bi_2Mo_2O_9$.

The structure of $Bi_2Mo_2O_9$ is shown in Figs. 1 and 2. Table I contains a summary of the crystal data; the positional and thermal parameters are given in Table II, and

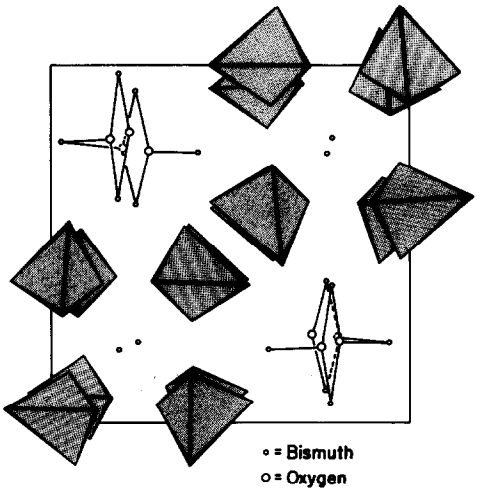

FIG. 2. Structure of $Bi_2Mo_2O_9$ projected in the a–c plane. The unit cell is outlined with a as the vertical axis. The MoO_4 groups are shown as tetrahedra. The Bi_3O_2 chains along the b axis are shown.

TABLE I

DATA FOR THE X-RAY DIFFRACTION STUDY FOR $Bi_2Mo_2O_9$

Formula		$Bi_2Mo_2O_9$
Formula weight		753.83
Crystal system		Monoclinic
Space group		$P2_1/n$ (No. 13)
Unit cell	a	11.972(3)
	b	10.813(4)
	c	11.899(2)
	β	90.13(2)°
	V	1540.4 Å^3
Z		8
Absorption coefficient		464.2 cm^{-1}
Calculated density		6.501 g/cm^3
Radiation λ(Mo$K\alpha$)		0.71069 Å
Monochromater		Graphite
Crystal dimension		0.100 × 0.033 × 0.033 mm
No. of independent reflections		2711
No. of reflection $F^2 > 2\sigma(F^2)$		1654
No. of variable refined		146
R		0.051
R_w		0.057
Error in observation of unit weight		1.728

the interatomic distances are in Tables III and IV.

Description of Structure

All the Mo atoms are in more or less ideal MoO_4 tetrahedral configuration; the Mo–O distances are nearly equal with an average value of 1.756 Å, compared to 1.77 Å expected from the tabulation of Shannon and Prewitt (*11*). The O–Mo–O angles have an average value of 109.5°, essentially that expected for tetrahedral coordination. The next nearest O atoms are 2.8 Å away. All 4 Bi atoms are 8-coordinated, but Bi(3) distinguishes itself from the others in the square antiprismatic coordination with a relatively small spread in the eight Bi–O distances (averaged to 2.456 Å). This is similar to the BiO_8 polyhedron in $BiVO_4$ (*12*).

The coordinations of Bi(1), Bi(2), and Bi(4) are irregular but similar to each other and typical of lone pair cations. These three Bi atoms are each bonded to two oxygens at very short distances [O(1) and O(2)] which are not shared with any Mo atoms. Together these bismuth and oxygen atoms form chains parallel to the *b* axis as illustrated in Fig. 2.

As previously mentioned, the $Bi_2Mo_2O_9$ structure can be viewed as an approximate body-centered arrangement of cations where $\frac{1}{9}$ of the cation positions are vacant. This leaves large cavities in the structure, which are surrounded by oxygens. Most oxygens in the $Bi_2Mo_2O_9$ structure are coordinated to three cations, but some of those in the vicinity of the cavities are coordinated to only two cations.

Discussion

The $Bi_2Mo_2O_9$ structure described by van der Elzen and Rieck (*6*) from their powder data is remarkably close to the correct structure. They were able to locate the metal atoms and suggest approximate locations for O atoms. However, their suggestion that the MoO_4 tetrahedra are strongly distorted, with the possibility of 5- to 6-coordination, is not substantiated.

Despite the similar catalytic properties of Bi_2MoO_6, $Bi_2Mo_2O_9$, and $Bi_2Mo_3O_{12}$, their structures are very different. The structure of α-Bi_2MoO_6[3] is composed of Bi_2O_2 layers, where bismuth shows a pronounced lone-pair type bonding, and MoO_4 layers with octahedra of molybdenum sharing corners. The structure of $Bi_2Mo_3O_{12}$ is composed of isolated MoO_4 tetrahedra and bismuth atoms coordinated to oxygen much as in

[3] α-Bi_2MoO_6 refers to the low-temperature form of Bi_2MoO_6 which contains octahedral molybdenum. The high-temperature form, β-Bi_2MoO_6, contains tetrahedral molybdenum. Regrettably, the catalyst literature frequently refers to the Bi_2MoO_6 composition as γ-bismuth molybdate.

TABLE II

POSITIONAL AND THERMAL PARAMETERS AND THEIR ESTIMATED STANDARD DEVIATIONS

Atom	x	y	z	$B(1,1)$	$B(2,2)$	$B(3,3)$	$B(1,2)$	$B(1,3)$	$B(2,3)$
Bi 1	−0.10020(9)	0.1209(2)	0.7564(1)		0.00185(10)	0.00163(9)	0.0002(2)	−0.0003(1)	−0.0011(2)
Bi 2	0.60326(9)	0.1229(2)	0.7583(1)		0.00201(10)	0.00142(8)	0.0000(2)	−0.0005(1)	0.0005(2)
Bi 3	0.25585(11)	0.1232(2)	0.7585(1)		0.00155(9)	0.00122(8)	0.0003(2)	−0.0006(1)	0.0000(2)
Bi 4	0.25301(9)	0.1228(1)	0.4122(1)		0.00142(9)	0.00097(8)	0.0004(3)	−0.0003(1)	0.0000(3)
Mo 1	−0.0827(2)	0.1230(4)	0.8722(2)	0.00104(7)	0.0016(2)	0.0008(2)	0.0003(5)	−0.0007(3)	0.0003(5)
Mo 2	−0.0784(2)	0.1250(4)	0.4163(2)	0.0010(2)	0.0016(2)	0.0013(2)	−0.0008(5)	−0.0007(3)	0.0008(5)
Mo 3	0.5893(2)	0.1272(4)	0.0814(2)	0.0019(2)	0.0019(3)	0.0014(2)	−0.0005(5)	−0.0002(3)	0.0003(5)
Mo 4	0.5791(2)	0.1321(4)	0.4156(2)	0.0011(2)	0.0023(3)	0.0019(2)	−0.0007(5)	−0.0002(3)	0.0010(5)
O1	0.252(2)	0.261(2)	0.285(2)	1.3(5)					
O2	0.255(2)	0.493(2)	0.227(2)	1.1(5)					
O3	0.409(2)	0.257(2)	0.689(2)	1.3(5)					
O4	0.326(2)	0.259(2)	0.901(2)	1.1(5)					
O5	0.105(2)	0.437(3)	0.447(2)	1.6(5)					
O6	0.101(2)	0.251(2)	0.815(2)	1.0(4)					
O7	0.405(2)	0.444(2)	0.048(2)	1.9(4)					
O8	0.093(2)	0.494(3)	0.684(2)	1.4(5)					
O9	0.194(2)	0.260(2)	0.596(2)	1.2(5)					
O10	0.097(2)	0.313(3)	0.050(2)	1.8(5)					
O11	0.403(2)	0.308(2)	0.454(2)	0.9(4)					
O12	0.056(2)	0.187(2)	0.388(2)	0.7(4)					
O13	0.044(2)	0.046(2)	0.112(2)	0.9(4)					
O14	0.447(2)	0.066(2)	0.383(2)	1.1(5)					
O15	0.399(2)	0.495(3)	0.820(2)	1.4(5)					
O16	0.962(2)	0.300(30	0.599(2)	1.5(5)					
O17	0.177(2)	0.489(2)	0.904(2)	1.2(5)					
O18	0.192(2)	0.988(3)	0.903(2)	1.7(5)					

Note. The form of the anisotropic thermal parameter is: exp[−($B(1,1)$*H*H + $B(2,2)$*K*K + $B(3,3)$*L*L + $B(1,2)$*H*K + $B(1,3)$*H*L + $B(2,3)$*K*L)].

TABLE III

INTERATOMIC DISTANCES CENTERED AROUND THE METAL ATOMS

Bi(1)–O(2)	2.151(20)	Bi(2)–O(1)	2.196(21)
Bi(1)–O(1)	2.212(21)	Bi(2)–O(2)	2.241(21)
Bi(1)–O(11)	2.474(19)	Bi(2)–O(5)	2.337(21)
Bi(1)–O(13)	2.477(19)	Bi(2)–O(10)	2.575(22)
Bi(1)–O(7)	2.577(19)	Bi(2)–O(12)	2.641(19)
Bi(1)–O(16)	2.793(19)	Bi(2)–O(14)	2.714(19)
Bi(1)–O(6)	2.868(18)	Bi(2)–O(8)	2.813(19)
Bi(1)–O(15)	2.919(21)	Bi(2)–O(3)	2.861(19)
Bi(3)–O(8)	2.382(19)	Bi(4)–O(1)	2.129(23)
Bi(3)–O(18)	2.389(21)	Bi(4)–O(2)	2.172(23)
Bi(3)–O(4)	2.396(19)	Bi(4)–O(14)	2.431(18)
Bi(3)–O(6)	2.407(19)	Bi(4)–O(12)	2.478(17)
Bi(3)–O(3)	2.479(20)	Bi(4)–O(9)	2.736(19)
Bi(3)–O(15)	2.496(19)	Bi(4)–O(11)	2.737(19)
Bi(3)–O(9)	2.540(20)	Bi(4)–O(7)	2.745(19)
Bi(3)–O(17)	2.555(20)	Bi(4)–O(17)	2.750(19)
Average	2.456 ± 0.071		
Mo(1)–O(13)	1.758(18)	Mo(2)–O(4)	1.708(19)
Mo(1)–O(11)	1.763(19)	Mo(2)–O(7)	1.747(19)
Mo(1)–O(3)	1.772(21)	Mo(2)–O(15)	1.747(19)
Mo(1)–O(18)	1.775(21)	Mo(2)–O(12)	1.767(18)
Average	1.767 ± 0.008	Average	1.742 ± 0.205
Averaged angle	109.5 ± 4.3°	Averaged angle	109.5 ± 4.0°
Mo(3)–O(16)	1.730(21)	Mo(4)–O(10)	1.717(22)
Mo(3)–O(5)	1.752(21)	Mo(4)–O(17)	1.759(20)
Mo(3)–O(9)	1.761(20)	Mo(4)–O(6)	1.768(20)
Mo(3)–O(8)	1.798(21)	Mo(4)–O(14)	1.772(18)
Average	1.760 ± 0.028	Average	1.754 ± 0.025
Averaged angle	109.5 ± 3.8°	Averaged angle	109.5 ± 4.9°

TABLE IV

INTERATOMIC DISTANCES CENTERED AROUND O ATOMS

O(1) –Bi(3)	2.129(23)	O(2) –Bi(1)	2.151(20)
O(1) –Bi(2)	2.196(21)	O(2) –Bi(4)	2.172(23)
O(1) –Bi(4)	2.212(21)	O(2) –Bi(2)	2.241(21)
O(3) –Mo(1)	1.772(21)	O(4) –Mo(2)	1.708(19)
O(3) –Bi(3)	2.479(20)	O(4) –Bi(3)	2.396(19)
O(3) –Bi(2)	2.861(19)		
O(5) –Mo(3)	1.752(21)	O(6) –Mo(4)	1.768(20)
O(5) –Bi(2)	2.337(21)	O(6) –Bi(3)	2.407(19)
		O(6) –Bi(1)	2.868(18)
O(7) –Mo(2)	1.747(19)	O(8) –Mo(3)	1.798(21)
O(7) –Bi(1)	2.577(19)	O(8) –Bi(3)	2.382(19)
O(7) –Bi(4)	2.745(19)	O(8) –Bi(2)	2.813(19)
O(9) –Mo(3)	1.761(20)	O(10)–Mo(4)	1.717(22)
O(9) –Bi(3)	2.540(20)	O(10)–Bi(2)	2.575(22)
O(9) –Bi(4)	2.736(20)		
O(11)–Mo(1)	1.763(19)	O(12)–Mo(2)	1.767(18)
O(11)–Bi(1)	2.474(19)	O(12)–Bi(4)	2.478(17)
O(11)–Bi(4)	2.737(19)	O(12)–Bi(2)	2.141(19)
O(13)–Mo(1)	1.758(18)	O(14)–Mo(4)	1.772(18)
O(13)–Bi(1)	2.474(19)	O(14)–Bi(4)	2.431(18)
		O(14)–Bi(2)	2.714(19)
O(15)–Mo(2)	1.747(21)	O(16)–Mo(3)	1.730(21)
O(15)–Bi(3)	2.496(19)	O(16)–Bi(1)	2.793(19)
O(15)–Bi(1)	2.919(21)		
O(17)–Mo(4)	1.759(20)	O(18)–Mo(1)	1.775(21)
O(17)–Bi(3)	2.555(20)	O(18)–Bi(3)	2.389(21)
O(17)–Bi(4)	2.750(19)		

$BiVO_4$. Thus, the $Bi_2Mo_2O_9$ structure contains features of the Bi_2MoO_6 and $Bi_2Mo_3O_{12}$ structures. The molybdenum coordination is essentially the same as in $Bi_2Mo_3O_{12}$ except the tetrahedra are more regular. Some bismuth in $Bi_2Mo_2O_9$ is coordinated much the same as in $Bi_2Mo_3O_{12}$, but most of the bismuth has a coordination more similar to that found in α-Bi_2MoO_6. However, the strong bismuth oxygen bonding in α-Bi_2MoO_6 leads to layer formation whereas in $Bi_2Mo_2O_9$ this bonding leads to the formation of chains only.

Acknowledgments

The crystals of $Bi_2Mo_2O_9$ were grown by A. Ferretti. E. P. Moore and J. L. England assisted in the crystallographic work.

References

1. B. C. Gates, J. R. Katzer, and G. C. A. Schuit, "Chemistry of Catalytic Processes," McGraw–Hill, New York (1979).
2. H.-Y. Chen, *Mater Res. Bull.* **14,** 1583 (1979).
3. A. F. van den Elzen and G. D. Rieck, *Acta Crystallogr. Sect. B* **29,** 2436 (1973).
4. A. F. van den Elzen and G. D. Rieck, *Acta Crystallogr. Sect. B.* **29,** 2433 (1973).
5. R. K. Grasselli, J. D. Burrington, and J. F. Brazdil, *Faraday Discuss. Chem. Soc.* **72,** 203 (1982).
6. A. F. van den Elzen and G. D. Rieck, *Mater. Res. Bull.* **10,** 1163 (1975).
7. B. Grybowska, J. Haber, and J. Komorek, *J. Catal.* **25,** 25 (1972).
8. L. Ya. Erman and E. L. Galperin, *Russ. J. Inorg. Chem. (Engl. Transl.)* **15,** 441 (1970).
9. B. A. Frenz, "The Enraf-Nonius CAD4 SDP, a Real-Time System for Concurrent X-Ray Data Collection and Crystal Structure Determination," Computing in Crystallography (H. Schenk, R. Orthaf-Hazechamp, H. von Konigueld, and G. C. Gassio, Eds.), pp. 64–71, Delft Univ. Press, Delft, Holland (1978).
10. "International Tables for X-Ray Crystallography," Vol. VI, Tables 2.2B and 2.3.1, Kynoch Press, Birmingham, England (1974).
11. R. D. Shannon and C. T. Prewitt, *Acta Crystallogr. Sect. B* **25,** 925 (1969).
12. A. W. Sleight, H.-Y. Chen, A. Ferretti, and D. E. Cox, *Mater. Res. Bull.* **14,** 157 (1979).